

Electronic Supplementary Information

## **The True Liquid Crystal Phases of 2D Polymeric Carbon Nitride and Macroscopic Assembled Fibers**

Ji-Yoon Song,<sup>‡ac</sup> Hui-ju Kang,<sup>‡a</sup> Jong Chan Won,<sup>bd</sup> Yun Ho Kim,<sup>\*bd</sup> Young-Si Jun<sup>\*a</sup> and Hyeon Su Jeong<sup>\*c</sup>

<sup>a</sup>School of Chemical Engineering, Chonnam National University, 77 Yongbongro, Buk-gu, Gwangju 61186, Republic of Korea

<sup>b</sup>Department Advanced Materials Division, Korea Research Institute of Chemical Technology (KRICT), Daejeon 34114, Republic of Korea

<sup>c</sup>Institute of Advanced Composite Materials, Korea Institute of Science and Technology (KIST), Wanju-gun 55324, Republic of Korea

<sup>d</sup>Advanced Materials and Chemical Engineering, KRICT School, University of Science and Technology, Daejeon 34113, Republic of Korea

## Table of Contents

### Experimental

**Fig. S1** Cooperative assembly of melamine and tri-thiocyanuric acid via hydrogen bonding to give macroscopic organic crystal MTCA. a) scheme of formation of MTCA from precursors, b) SEM image and c) XRD pattern of MTCA.

**Fig. S2** Turbiscan data of MTCA-g-CN/SA98 at the concentration of 2 mg mL<sup>-1</sup> for 24 h.

**Fig. S3** a) Powder XRD patterns of DCDA-g-CN and MTCA-g-CN: d-spacing and stacking layer numbers calculated by (002) peak and Scherer equation are listed in Table. SEM images of b) MTCA and c) DCDA with insets that show anisotropy (length/width) in lateral plane.

**Fig. S4** a) POM results for phase changes during 100 °C heating and cooling to room temperature of MTCA-g-CN/SA98 solution at 550 mg mL<sup>-1</sup>, b) Schematic experimental setup of 2D-SAXD. 2D SAXD patterns at c) RT and d) 100 °C, e) 1D profiles from c) and d) averaged from -35° to 20° with the radial width of the integrated scattered intensity.

**Fig. S5** a) POM image and b) OM image of MTCA-g-CN/SA95 at the concentration of 700 mg mL<sup>-1</sup>.

**Fig. S6** Characterization of MTCA-g-CN. a) Photocatalytic hydrogen evolution rates under AM 1.5G condition, b) XRD patterns, c) DRS UV-vis spectra, d) FT-IR, e) XPS and f) atomic contents from XPS.

**Movie S1.** Phenomenon of expansion of MTCA-g-CN after drop of SA98.

**Movie S2.** Rotating POM image of MTCA-g-CN/SA98 at the concentration of 550 mg mL<sup>-1</sup>.

**Movie S3.** Continuous fiberization of MTCA-g-CN fiber in coagulation bath.

## Experimental

**Preparation of DCDA-g-CN.** DCDA-g-CN was gained by calcination of 20 g of DCDA in the box furnace into glass beaker and cover glass at 550 °C with ramp time of 4 h and kept for 4 h and naturally cooled to RT.

**Preparation of MTCA-g-CN.** MTCA-g-CN was synthesized as published paper.<sup>1</sup> 0.5 g of melamine and 0.51 g of tri-thiocyanuric acid were dissolved in 30 mL of dimethyl sulfoxide (DMSO). And the solution was poured into the 30 mL of deionized water forming light yellow precipitation. Formed emulsion was washed with vacuum filtration washing deionized water to remove residual DMSO. The precipitation was dried in the dry oven at 120 °C overnight to evaporate water and light-yellow powder was gained, called MTCA. MTCA-g-CN was gained by calcination of MTCA in the tube furnace into the boat-shaped alumina crucible to 550 °C with ramp time 4 h and kept for 4 h under N<sub>2</sub>. The furnace was naturally cooled to RT and gained MTCA-g-CN.

**Preparation of LC solution.** 1 mL of sulfuric acid (95, 98 and 110%) was poured in the glass vial with  $x$  g of powder of graphitic carbon nitride. And it was stirred in the oil bath of 90 °C for 2 hr.

**Fiberization.** Prepared LC solution was inhaled from glass vial to the syringe and exhaled using spinning needle (0.41 mm of inner diameter) in the acetone as coagulation bath.

**Characterization.** The structures of MTCA, DCDA-g-CN and MTCA-g-CN were analyzed by scanning electron microscopy (FE-SEM, EX-200, 15.0 kV, Hitachi, Tokyo, Japan). FT-IR spectra were recorded by FT-IR spectroscopy (FT/IR-4100, Jasco) and <sup>13</sup>C CP/MAS solid NMR were analyzed by ECZ400R, JEOL, 400 MHz system. XRD patterns were recorded on a D/MAX Ultima III (Rigaku, Japan) with Cu K $\alpha$  (Cu-1.6 kW,  $\lambda = 0.154$  nm) radiation. POM

and OM images were obtained by polarized optical microscopy (Nikon Eclipse LV100N POL). Small angle X-ray scattering (SAXS) experiments (3C beamline of the Pohang Accelerator Laboratory (PAL)) was conducted to observe LC phase.

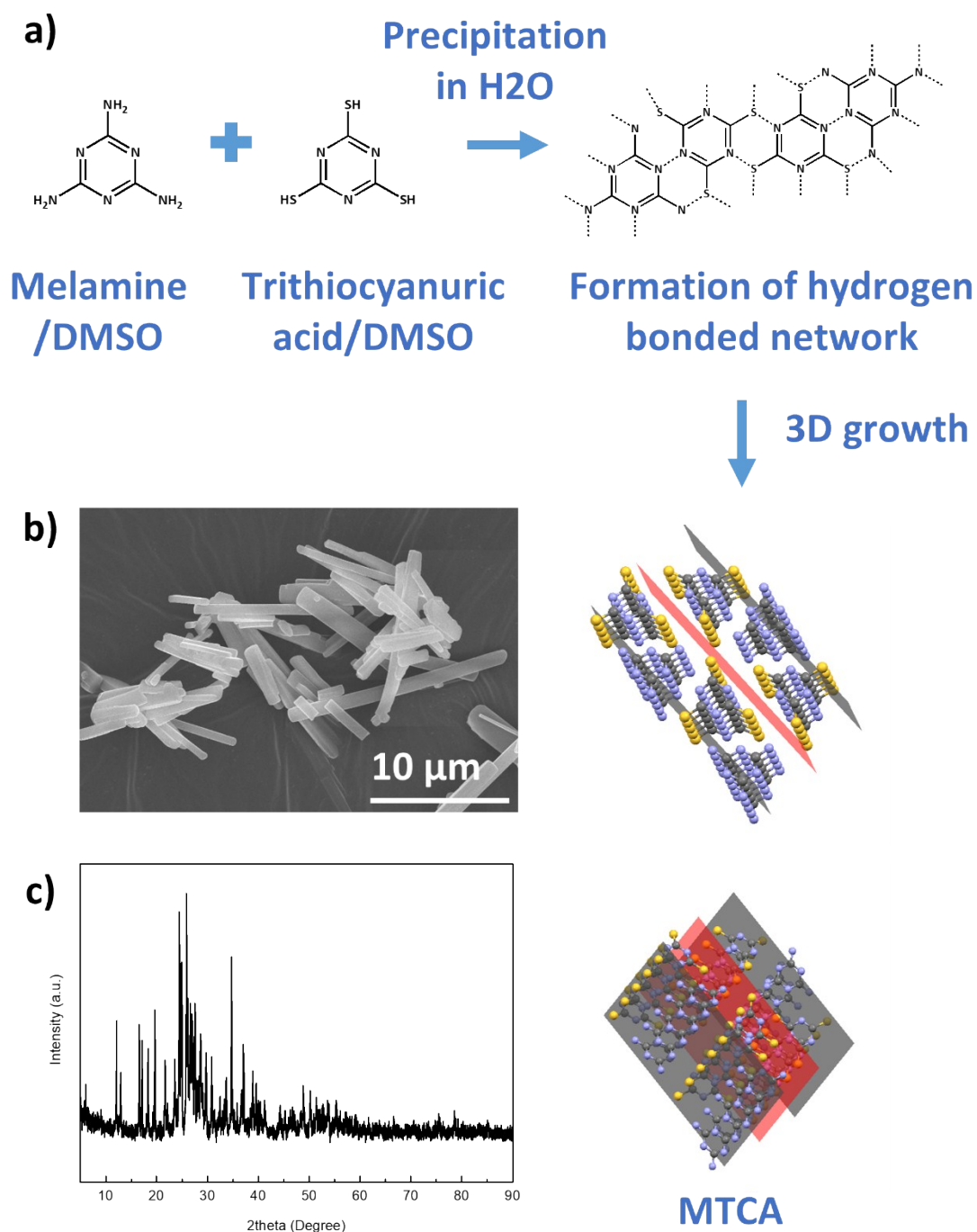


**Fig. S1** Cooperative assembly of melamine and tri-thiocyanuric acid via hydrogen bonding to give macroscopic organic crystal MTCA. a) scheme of formation of MTCA from precursors, b) SEM image and c) XRD pattern of MTCA.

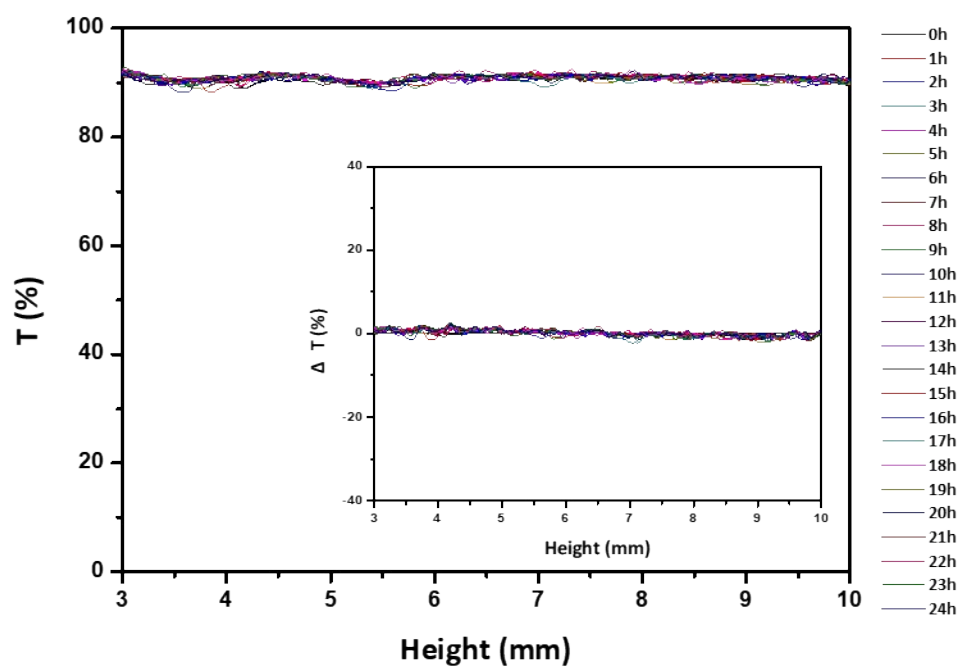


**Fig. S2** Turbiscan data of MTCA-g-CN/SA98 at the concentration of 2 mg mL<sup>-1</sup> for 24 h. (inset: differential value of transmittance)

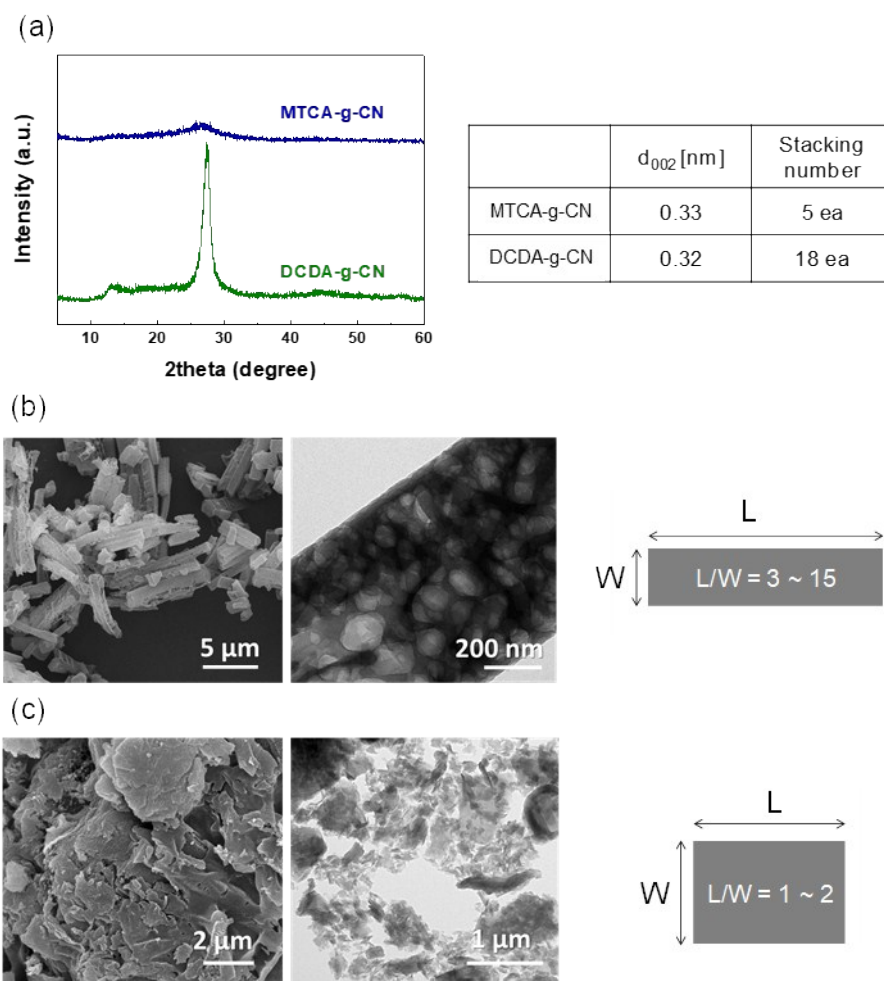


**Fig. S3** a) Powder XRD patterns of DCDA-g-CN and MTCA-g-CN: d-spacing and stacking layer numbers calculated by (002) peak and Scherrer equation are listed in Table. SEM images of b) MTCA and c) DCDA with insets that show anisotropy (length/width) in lateral plane.

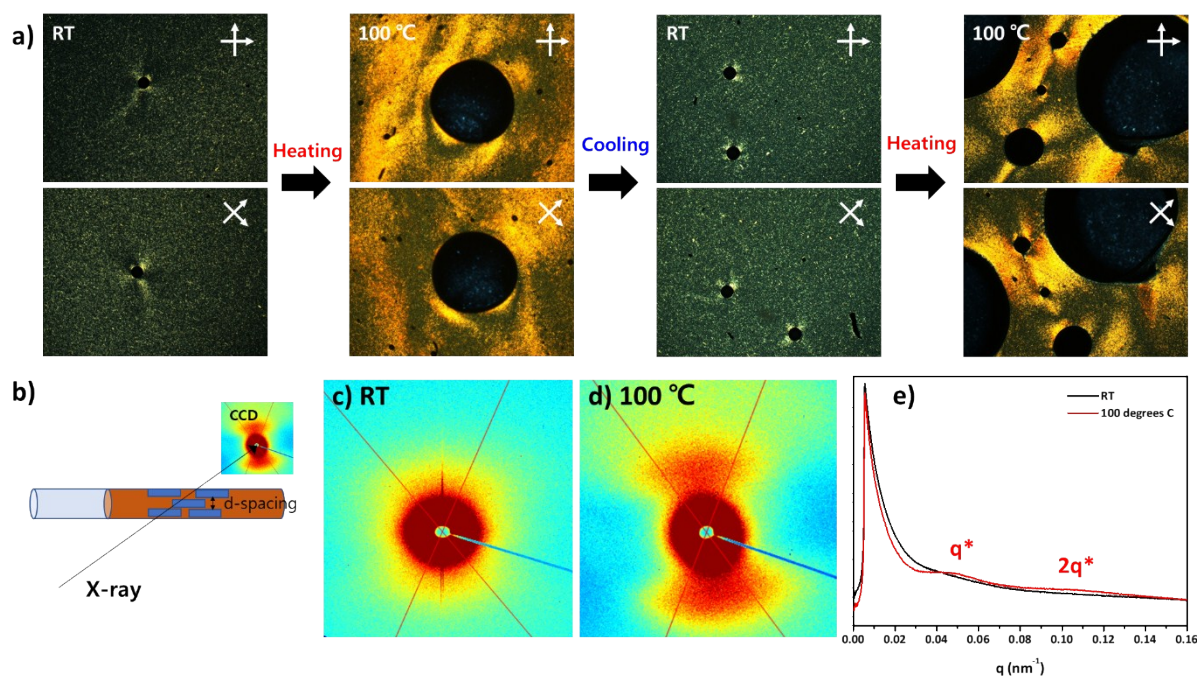


**Fig. S4** a) POM results for phase changes during 100 °C heating and cooling to room temperature of MTCA-g-CN/SA98 solution at  $550\text{mg mL}^{-1}$ , b) Schematic experimental setup of 2D-SAXD. 2D SAXD patterns at c) RT and d) 100 °C, e) 1D profiles from c) and d) averaged from  $-35^\circ$  to  $20^\circ$  with the radial width of the integrated scattered intensity.



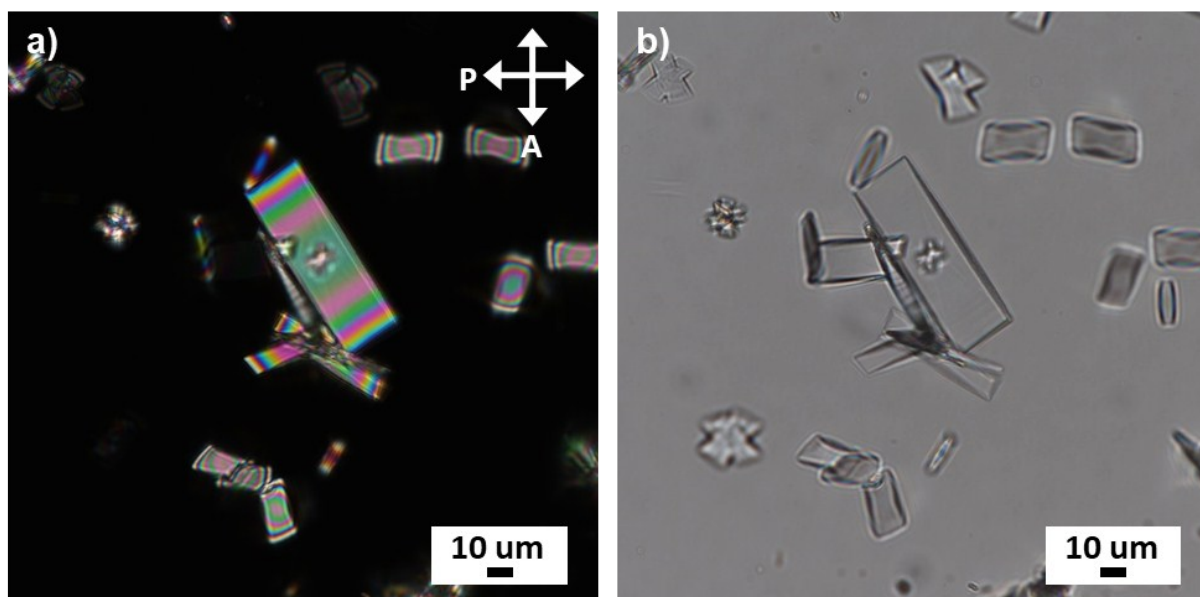


**Fig. S5** a) POM image and b) OM image of MTCA-g-CN/SA95 at the concentration of 700 mg mL<sup>-1</sup>.

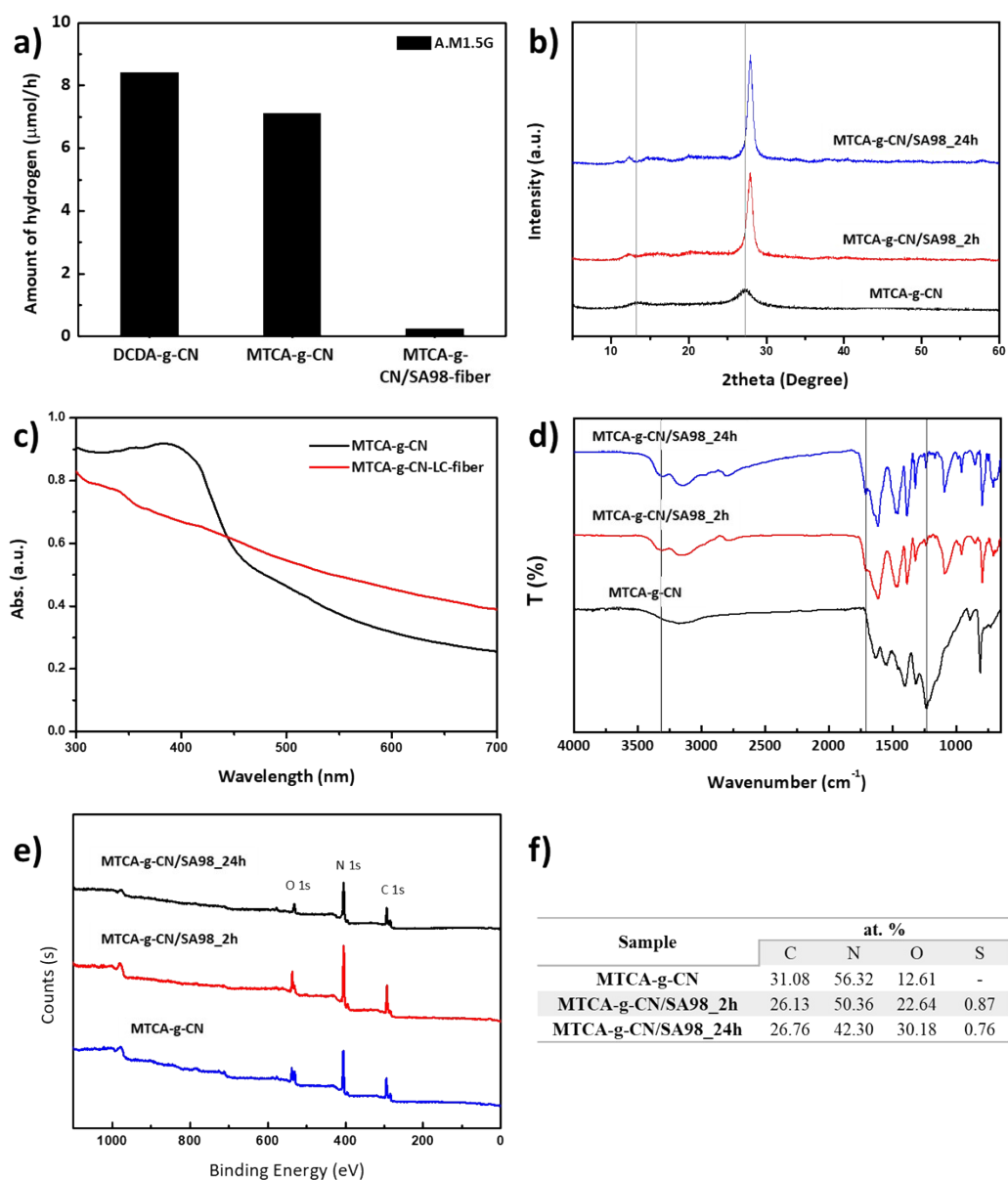


**Fig. S6** Characterization of MTCA-g-CN. a) Photocatalytic hydrogen evolution rates under AM 1.5G condition, b) XRD patterns, c) DRS UV-vis spectra, d) FT-IR, e) XPS and f) atomic contents from XPS.

We provide other properties through photocatalytic activity via hydrogen evolution reaction. MTCA-g-CN/SA98-fiber produces negligible hydrogen even under AM 1.5G condition after dissolution/precipitation (Fig. S6a). Depolymerization or decomposition into monomers

probably leads to 1) better packing of the residual materials due to decrease of steric hindrance, shifting of a peak around 27 degree to a higher scattering angle in power XRD diffraction patterns (Fig. S6b), and 2) loss of optoelectronic properties, losing light absorption centered at 400 nm as can be seen in diffuse reflectance UV-vis spectra before and after dissolution/precipitation (Fig. S6c). Exfoliation and spontaneous dissolution of MTCA-g-CN is achieved at the cost of structural decomposition by highly oxidative, high-concentrated sulfuric acid.<sup>2</sup> Such reaction is initiated at  $-\text{NH}_x$  ( $x=1$  or  $2$ ) sites, conversion of which into  $-\text{OH}$  and then into  $\text{C}=\text{O}$  via Keto-Enol tautomerization is proved by a peak around  $3300\text{ cm}^{-1}$  and  $1700\text{ cm}^{-1}$ , respectively (Fig. S6d). Further decomposition of the tri-*s*-triazine moieties, meaning ring-opening reaction, is observed by disappearance of multiple peaks around  $1230\text{ cm}^{-1}$  corresponding to stretching vibrations of aromatic CN heterocycles.<sup>3</sup> The same trend can also be found in XPS spectra in Fig. S6e: the atomic content of O atom increases from 12.61% to 22.64 and 30.18% after 2 h and 24 h in high concentrated (98%) sulfur acid, while that of N decreases from 56.32 to 50.36% and 42.30% (Fig. S6f). The absence of photocatalytic performance is supposed that  $-\text{OH}$  or  $\text{C}=\text{O}$  terminal groups may not allow tight binding to Pt electrocatalyst for charge transfer either.

## References

1. Y. S. Jun, J. Park, S. U. Lee, A. Thomas, W. H. Hong and G. D. Stucky, *Angewandte Chemie International Edition*, 2013, **52**, 11083-11087.
2. Y. J. Zhang, A. Thomas, M. Antonietti and X. C. Wang, *Journal of the American Chemical Society*, 2009, **131**, 50-51.
3. J. S. Zhang, M. W. Zhang, L. H. Lin and X. C. Wang, *Angewandte Chemie-International Edition*, 2015, **54**, 6297-6301.